Atmos. Chem. Phys., 20, 7259–7269, 2020
https://doi.org/10.5194/acp-20-7259-2020

Atmospheric Chemistry and Physics
Open Access
EGU

Importance of gas-particle partitioning of ammonia in haze formation in the rural agricultural environment

Jian Xu[1], Jia Chen[1], Na Zhao[1], Guochen Wang[1], Guangyuan Yu[1], Hao Li[1], Juntao Huo[3], Yanfen Lin[3], Qingyan Fu[3], Hongyu Guo[4], Congrui Deng[1], Shan-Hu Lee[5], Jianmin Chen[1], and Kan Huang[1,2]

[1]Shanghai Key Laboratory of Atmospheric Particle Pollution and Prevention (LAP3),
Department of Environmental Science and Engineering, Fudan University, Shanghai, 200433, China
[2]Institute of Eco-Chongming (IEC), No.20 Cuiniao Road, Chen Jiazhen, Shanghai, 202162, China
[3]Shanghai Environmental Monitoring Center, Shanghai, 200030, China
[4]Cooperative Institute for Research in Environmental Sciences and Department of Chemistry,
University of Colorado, Boulder, Colorado 80309, USA
[5]Department of Atmospheric Science, University of Alabama in Huntsville, Huntsville, Alabama 35758, USA

Correspondence: Kan Huang (huangkan@fudan.edu.cn)

Received: 9 October 2019 – Discussion started: 13 January 2020
Revised: 10 May 2020 – Accepted: 25 May 2020 – Published: 23 June 2020

Abstract. Ammonia in the atmosphere is essential for the formation of fine particles that impact air quality and climate. Despite extensive prior research to disentangle the relationship between ammonia and haze pollution, the role of ammonia in haze formation in high ammonia-emitting regions is still not well understood. Aiming to better understand secondary inorganic aerosol (sulfate, nitrate, ammonium – SNA) formation mechanisms under high-ammonia conditions, 1-year hourly measurement of water-soluble inorganic species (gas and particle) was conducted at a rural supersite in Shanghai. Exceedingly high levels of agricultural ammonia, constantly around 30 $\mu g\,m^{-3}$, were observed. We find that gas-particle partitioning of ammonia ($\varepsilon(NH_4^+)$), as opposed to ammonia concentrations, plays a critical role in SNA formation during the haze period. From an assessment of the effects of various parameters, including temperature (T), aerosol water content (AWC), aerosol pH, and activity coefficient, it seems that AWC plays predominant regulating roles for $\varepsilon(NH_4^+)$. We propose a self-amplifying feedback mechanism associated with $\varepsilon(NH_4^+)$ for the formation of SNA, which is consistent with diurnal variations in $\varepsilon(NH_4^+)$, AWC, and SNA. Our results imply that a reduction in ammonia emissions alone may not reduce SNA effectively, at least at rural agricultural sites in China.

1 Introduction

Gas-phase ammonia (NH_3) in the environment not only fuels the eutrophication and acidification of ecosystems, but also plays key roles in atmospheric chemistry. NH_3 has been known to promote new particle formation both in the initial homogeneous nucleation and in subsequent growth (Ball et al., 1999; Zhang et al., 2011; Coffman and Hegg, 1995; Kirkby et al., 2011). Prior studies suggest that the SO_2 oxidation can be enhanced by the presence of NH_3 (Turšič et al., 2004; Wang et al., 2016; Benner et al., 1992). High levels of NH_3 can also promote secondary organic aerosol (SOA) formation (Na et al., 2007; Ortiz-Montalvo et al., 2013). As the main alkaline species in the atmosphere, NH_3 is expected to affect the acidity of clouds (Wells et al., 1998), fine particles (Liu et al., 2017; Guo et al., 2017b), and wet deposition (Ap-Simon et al., 1987) by neutralizing acidic species. The neutralized ammonium (NH_4^+) exclusively contributes to aerosol hygroscopicity especially in hazy periods (Liu et al., 2017; Ye et al., 2011). Serving as efficient catalysts for aerosol aldol condensation, ammonium has also been proved to contribute to radiative forcing (Noziere et al., 2010; Park et al., 2014). Most importantly, ammonium is among the major secondary inorganic aerosols (i.e., sulfate SO_4^{2-}, nitrate NO_3^-, and ammonium NH_4^+, denoted as SNA), which typically rivals the organics and can make up more than 50 % of $PM_{2.5}$

mass loadings (Wang et al., 2015a; Sun et al., 2014; Huang et al., 2014; Plautz, 2018; Schiferl et al., 2014). Despite the significant importance of SNA in hazy periods, the formation mechanism responsible, particularly the role of NH_3, remains highly controversial. Cheng et al. (2016) and Wang et al. (2016), for example, suggested that the near-neutral acidity, resulting from the NH_3-rich atmosphere, is vital for SNA formation. While Liu et al. (2017) and Guo et al. (2017b) demonstrated that the close to neutral state is unlikely even under conditions of excess NH_3. These findings collectively imply that the fundamental role of NH_3 in regulating aerosol acidity is still ambiguous, thus altering the SNA formation mechanism (Seinfeld and Pandis, 2012).

NH_3 emission sources include agricultural practices, on-road vehicles (Chang et al., 2016; Sun et al., 2017), and biomass burning (Lamarque et al., 2010; Paulot et al., 2017). Recent field measurements and modeling work reveal that agricultural practices (i.e., animal manure and fertilizer application) contribute to 80 %–90 % of total NH_3 emissions in China (Zhang et al., 2018; Kang et al., 2016; Huang et al., 2011). Globally, NH_3 emissions are projected to continue to rise along with an increasing demand in chemical fertilizers due to the growing human population (Erisman et al., 2008; Stewart et al., 2005) and in part because limiting NH_3 emissions has not been targeted as a priority in most countries. For example, even though stringent mitigation targets have been set for SO_2 and NO_x in China's 13th Five-Year Plan (2016–2020), slashing NH_3 emissions is not yet a prime concern in China. The sustained increase in NH_3 has been observed from space (Warner et al., 2017) and reported to deflect the mitigation efforts of SO_2 and NO_x emissions in east China (Fu et al., 2017).

Although agricultural NH_3 emission has been the subject of extensive research, previous studies have focused on densely populated or urban areas, where NH_3 was mostly "aged" and transformed into NH_4^+ downwind (Chang et al., 2016). Varying in location and time, the typical mass concentrations of NH_3 are on the order of several micrograms per cubic meter (Yao et al., 2006; Gong et al., 2013; Robarge et al., 2002; Chang et al., 2016; Phan et al., 2013), with extremely high levels of up to more than 20 $\mu g\,m^{-3}$ in the rural area of the North China Plain (Meng et al., 2018; Shen et al., 2011; Pan et al., 2018). Numerous studies highlighted the importance of NH_3 emissions from agricultural areas (Meng et al., 2018; Shen et al., 2011; Robarge et al., 2002; Wang et al., 2013; Nowak et al., 2012; Zhang et al., 2017; Warner et al., 2017), but the gas-particle conversion of agricultural NH_3 in rural regions and its subsequent impact on SNA formation has scarcely been reported and remains poorly understood.

In this study, we provide observational constraints on the abnormally high agricultural NH_3 emission at a rural site. We report our findings on the influence of $\varepsilon(NH_4^+)$ on SNA formation and discuss the decisive factors driving the $\varepsilon(NH_4^+)$.

2 Methods

2.1 Observation site

Field measurements of gases and fine particles were conducted over the course of a year from March 2017 to February 2018 at the Dongtan Wetland Park (31°32′ N, 121°58′ E; altitude: 12 m a.s.l.), which is approximately 50 km northeast of downtown Shanghai. The sampling site, illustrated in Fig. 1, was located on the east side of the island of Chongming, which is the largest eco-friendly island in China and the least developed district of Shanghai. The annual mean relative humidity (RH) is 78 % ± 19 % and the yearly mean temperature (T) is 16.3±9.9 °C. Although Chongming shares limited industrial and vehicle emissions compared to urban Shanghai, the level of fine particles on this island is slightly higher than the urban site (Fig. S1 in the Supplement). The overuse of nitrogen fertilizer has long been a large agricultural source of NH_3 emissions in China (Fan et al., 2011), with an increasing use especially in east-central China (Yang and Fang, 2015), where rice–wheat intercropping (similar to those in Chongming) was applied. Based on a 2011 agricultural NH_3 emission inventory in Shanghai, Chongming has the largest nitrogen fertilizer consumption among all the districts in Shanghai (Fang et al., 2015). According to the Multi-resolution Emission Inventory for China (MEIC, http://www.meicmodel.org/, last access: 27 July 2019) in 2016, nearly 94 % of NH_3 in Chongming came from the agricultural sector, accounting for 14 % of the total NH_3 emissions in Shanghai. In comparison, Chongming contributes only 6 % and 5 % of the total NO_x and SO_2 emissions in Shanghai, respectively (Table S1 in the Supplement). With the most intensive agriculture and 34 % of arable farmland area in Shanghai (Wen et al., 2011), atmospheric ammonium aerosols over the island of Chongming are mostly of agricultural origin. Therefore, this site is ideal for investigating the role of agricultural emissions of NH_3 in haze formation.

2.2 Measurements

Water-soluble samples of both gases (NH_3, SO_2, HCl, HNO_2, and HNO_3) and particles (NH_4^+, Na^+, K^+, Ca^{2+}, Mg^{2+}, Cl^-, NO_3^-, and SO_4^{2-}) were measured hourly using MARGA (Monitor for AeRosols and Gases in Air; ADI 2080, Metrohm Applikon B.V., Netherlands). Online sampling was conducted from March 2017 to February 2018 following the description in Kong et al. (2014). Briefly, air was drawn into a $PM_{2.5}$ cyclone inlet with a flow rate of 1 $m^3\,h^{-1}$ and passed through either a wet rotating denuder (gases) or a steam jet aerosol collector (aerosols). Subsequently, the aqueous samples were analyzed with ion chromatography. Meanwhile, mass loadings of $PM_{2.5}$ was determined by a Tapered Element Oscillating Microbalance coupled with Filter Dynamic Measurement System (TEOM 1405-F). The quality assurance/quality control (QA/QC) of these instruments

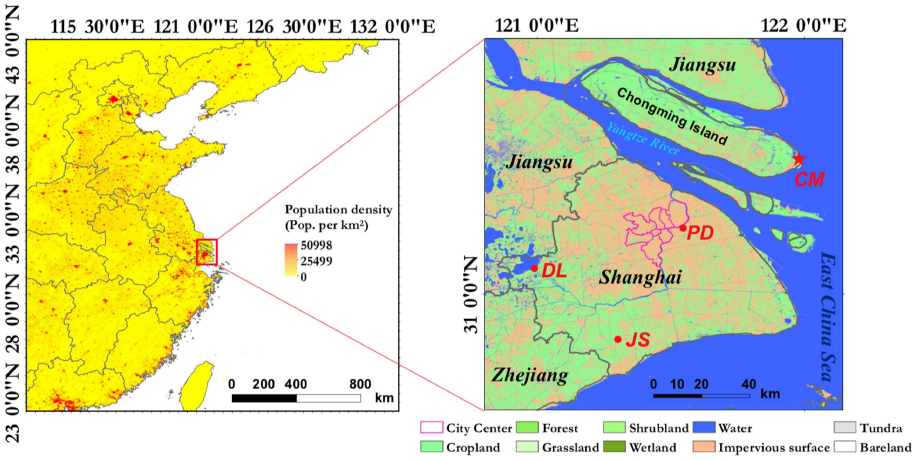

Figure 1. Location of the sampling site. Population density is color-coded in the left panel. The right panel shows the land cover in Shanghai (adapted from Peng et al., 2018). CM (Chongming) is the sampling site on the island of Chongming. JS (Jinshan) represents the source emission from a dairy farm in rural Shanghai. DL (Dianshan Lake) represents a regional transport region in the Yangtze River Delta. PD (Pudong) represents the urban site.

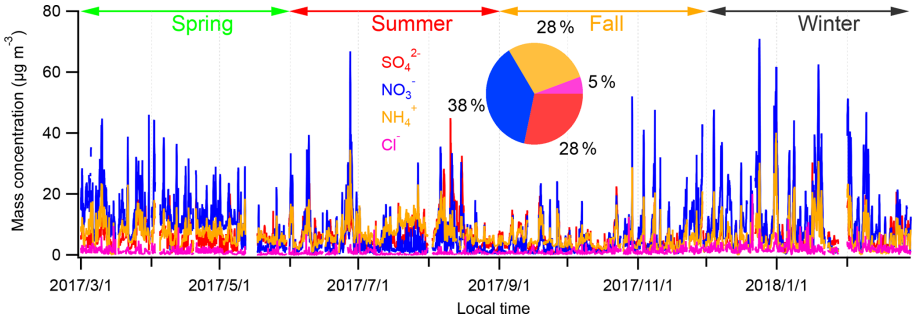

Figure 2. Time series of $PM_{2.5}$ species during the study period. The mass fraction of major $PM_{2.5}$ species is shown in the inserted pie chart.

was managed by professional staff at Shanghai Environmental Monitoring Center (SEMC) according to the *Technical Guideline of Automatic Stations of Ambient Air Quality in Shanghai* (HJ/T193-2005).

2.3 ISORROPIA-II modeling

The thermodynamic model ISORROPIA II (Fountoukis and Nenes, 2007) was used to predict the aerosol water content and pH. ISORROPIA was constrained in forward metastable mode by hourly mean measurements of Na^+, K^+, Mg^{2+}, Ca^{2+}, SO_4^{2-}, NH_3, NH_4^+, HNO_3, NO_3^-, HCl, and Cl^-, along with RH and T. The molality-based pH was a default output in the model. The model showed a good performance when predicting NH_3–NH_4^+ partitioning (Fig. S2).

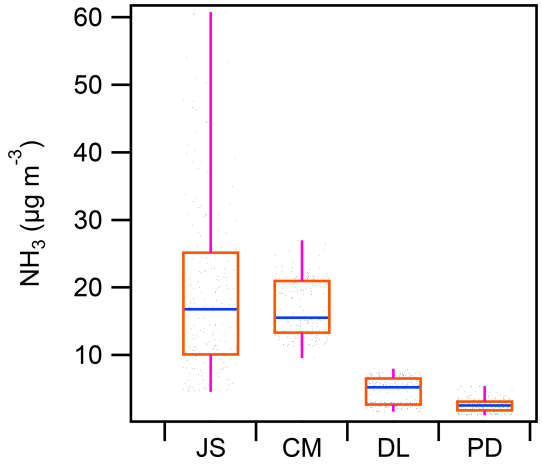

Figure 3. NH_3 at different sampling sites over the same period (From 18–27 January 2018). The locations of all sites are shown in Fig. 1. Scattered dots indicate raw data points.

Table 1. Statistical summary on mass concentrations of $PM_{2.5}$ species and NH_3.

Unit: $\mu g\,m^{-3}$	$PM_{2.5}$	SO_4^{2-}	NO_3^-	Cl^-	NH_4^+	NH_3
Non-haze	28.5 ± 16.9	5.6 ± 3.6	6.9 ± 6.6	1.1 ± 0.9	5.6 ± 3.3	32.2 ± 11.6
Haze	98.3 ± 37.2	13.3 ± 7.7	23.1 ± 14.5	2.2 ± 1.9	13.2 ± 6.6	32.3 ± 13.5

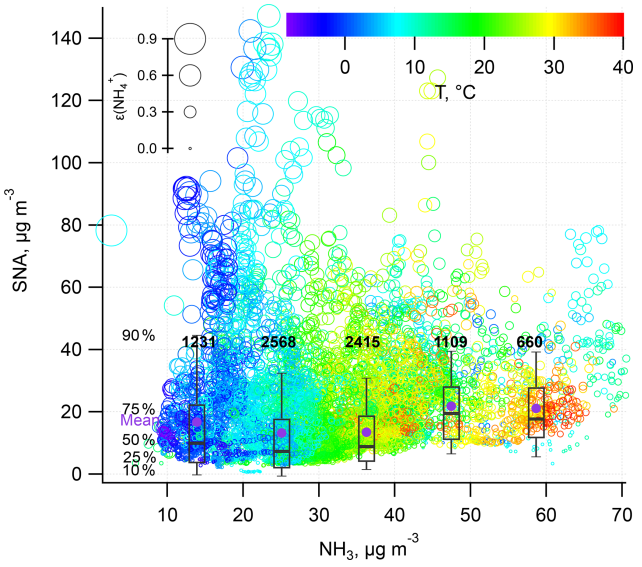

Figure 4. Secondary inorganic aerosol mass concentration in $PM_{2.5}$ (SNA refers to sulfate, nitrate, and ammonium) as a function of NH_3. The sizes of the void circles are scaled to the $\varepsilon(NH_4^+)$ and colored according to T. The number of data points in each NH_3 concentration bin is also shown.

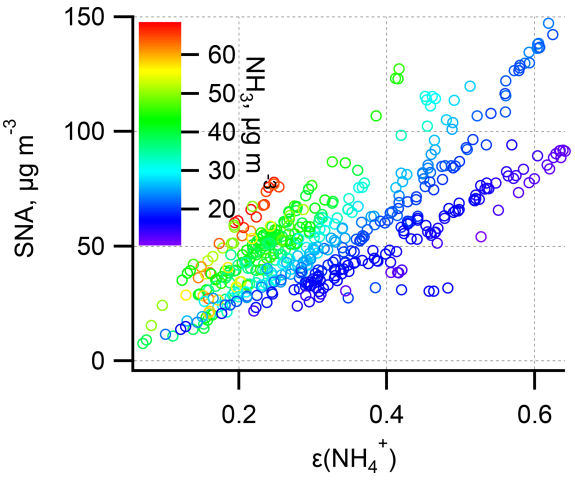

Figure 5. SNA mass concentration in $PM_{2.5}$ as a function of $\varepsilon(NH_4^+)$ during the haze period. The circles are colored according to the NH_3 mass concentration.

3 Results and discussion

3.1 Overview of 1-year continuous measurements at Chongming

Figure 2 shows the time series of hourly water-soluble $PM_{2.5}$ species during the study period. The mean concentration of NO_3^-, SO_4^{2-}, NH_4^+, and Cl^- over the entire study period was 8.4, 6.3, 6.3, and $1.2\,\mu g\,m^{-3}$. The haze period was defined as hourly mean $PM_{2.5}$ mass loadings higher than $75\,\mu g\,m^{-3}$, and the rest was non-haze periods. Table 1 gives the statistical summary of major aerosols during the haze and non-haze period. Clearly, the mass concentration of major $PM_{2.5}$ species (NO_3^-, SO_4^{2-}, NH_4^+, and Cl^-) increased during the haze period compared to those during the non-haze period. However, the concentration of NH_3 showed no significant change during these two periods. The mean mass concentration of SNA (sulfate, nitrate, and ammonium) was $49.0\,\mu g\,m^{-3}$, contributing to about 50.0 % of total $PM_{2.5}$ mass.

3.2 NH_3 levels and its link to secondary inorganic aerosol

Figure 3 shows that the mean concentration of NH_3 at Chongming (CM: $17.0 \pm 4.2\,\mu g\,m^{-3}$) was more than 3 times higher than at an urban site in Shanghai (PD: $2.5 \pm 0.9\,\mu g\,m^{-3}$) and a representative regional transport region (DL: $4.6 \pm 2.0\,\mu g\,m^{-3}$) in the Yangtze River Delta. The level of NH_3 at Chongming was even close to that observed inside a typical dairy farm (JS: $19.4 \pm 12.6\,\mu g\,m^{-3}$), which was dominated by livestock emissions. Thus, it is interesting to investigate how the formation of secondary inorganic aerosols is impacted by this abnormally high level of NH_3.

Figure 4 indicates the response of SNA mass concentrations to NH_3 is nonlinear. Higher NH_3 sometimes corresponds to even lower SNA mass concentrations. Statistically, the mean SNA concentration in each bin of NH_3 does not show significant difference. This is at odds with the traditional view that higher concentrations of precursors usually result in elevated inorganic aerosols (Nowak et al., 2010). Although the abundance of SNA is related to the alkaline gaseous precursor (e.g., NH_3), the question of whether the ambient condition (e.g., RH and T) and acid precursors (i.e., SO_2 and NO_x) favor the conversion of precursors into particles or not is equally important, if not more so. For example, the urban areas show higher SNA levels than the rural region, while a lower NH_3 mixing ratio was observed (Wu et

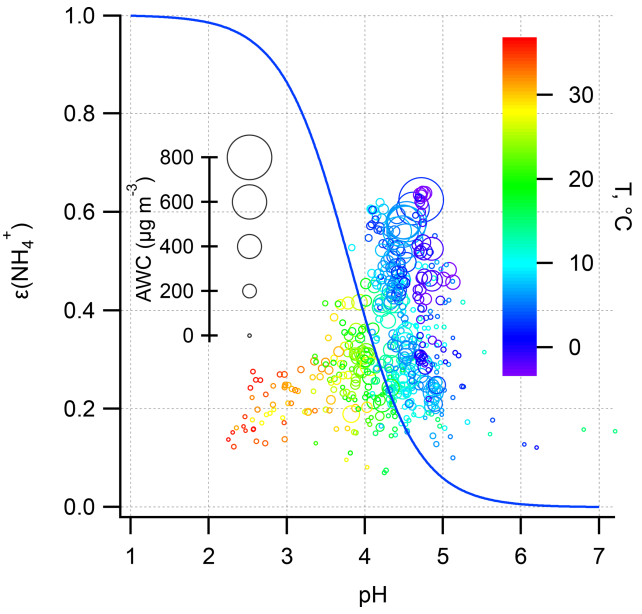

Figure 6. $\varepsilon(NH_4^+)$ as a function of pH during the haze period. The sizes of the void circles are scaled to AWC and colored according to T. The blue curve was calculated based on the mean T (10 °C), AWC (100 μg m^{-3}), and activity coefficient ratio of $\frac{\gamma_{H^+}}{\gamma_{NH_4^+}}$. The mean $\frac{\gamma_{H^+}}{\gamma_{NH_4^+}}$ for the haze period is 4.0 ± 2.6 ($\pm 1\sigma$).

al., 2016; Wang et al., 2015b). Previous field measurements suggest that rural NH_4^+ levels were more sensitive to acidic gases than to the NH_3 availability (Shen et al., 2011; Robarge et al., 2002). Therefore, the level of NH_3 concentration is not the determining factor for the formation of secondary inorganic aerosols.

3.3 The role of $\varepsilon(NH_4^+)$

In this regard, we further investigate the relationship between the gas-particle partitioning of ammonia ($\varepsilon(NH_4^+)$, defined as the molar ratio between particle phase ammonia (NH_4^+) and total ammonia ($NH_x = NH_3 + NH_4^+$)) and SNA during the haze period. The haze period is defined as hourly mean $PM_{2.5}$ mass loadings higher than 75 μg m^{-3}.

As shown in Fig. 5, it is obvious that SNA in $PM_{2.5}$ is almost linearly correlated with $\varepsilon(NH_4^+)$. Higher $\varepsilon(NH_4^+)$ results in higher SNA concentrations. In addition, under the same $\varepsilon(NH_4^+)$ conditions, higher NH_3 promotes stronger formation of SNA. Thus, NH_3 and $\varepsilon(NH_4^+)$ collectively determine the haze formation potential. The level of NH_3 can be regarded as a proxy of NH_3 emission intensity, which is source dependent. As for $\varepsilon(NH_4^+)$, it represents the relative abundance of gaseous NH_3 and particulate ammonium. The shift between the two phases is controlled by various factors such as the ambient environmental conditions. Previous study shows that elevated RH and acidic gas levels favor the shift in NH_3 towards the particulate phase at an urban site; thereby a lower $[NH_3] : [NH_4^+]$ ratio was observed (Wei et al., 2015). In this study, it is also observed that higher $\varepsilon(NH_4^+)$ values coincide with heightened RH, SO_2, and NO_x.

Based on the above results, the elucidation of the driving factors determining $\varepsilon(NH_4^+)$ is of great importance to explore the formation mechanism of haze. Theoretically, $\varepsilon(NH_4^+)$ is determined by NH_3, NH_4^+, and the equilibrium between NH_3 and NH_4^+. Assuming NH_3 and NH_4^+ are in thermodynamic equilibrium, the following equation can be obtained.

$$H^+ + NH_{3(g)} \leftrightarrow NH_4^+ \quad \text{(R1)}$$

The equilibrium constant $H^*_{NH_3}$ is equal to the Henry's constant of NH_3 divided by the acid dissociation constant for NH_4^+ (Clegg et al., 1998). $\varepsilon(NH_4^+)$ can be analytically calculated as detailed in Guo et al. (2017a) via the following equation:

$$\varepsilon(NH_4^+) = \frac{[NH_4^+]}{[NH_x]} \cong \frac{\frac{\gamma_{H^+}\,10^{-pH}}{\gamma_{NH_4^+}} H^*_{NH_3} W_i RT \times 0.987 \times 10^{-14}}{1 + \frac{\gamma_{H^+}\,10^{-pH}}{\gamma_{NH_4^+}} H^*_{NH_3} W_i RT \times 0.987 \times 10^{-14}}. \quad (1)$$

Here, $[NH_4^+]$ is the molar concentration of NH_4^+ (mole m^{-3}). γ is the activity coefficient, which is extracted from the ISORROPIA II model to account for the non-ideality solution effect. $H^*_{NH_3}$ (atm^{-1}) represents the molality-based equilibrium constant, which is T dependent and can be determined using Eq. (12) in Clegg et al. (1998). W_i (μg m^{-3}) is the aerosol water content predicted by ISORROPIA-II. R (J mole^{-1} K^{-1}) is the universal gas constant. T (K) is ambient temperature, and 0.987×10^{-14} is the conversion multiplication factors from standard atmosphere and microgram to SI units.

In Fig. 6, the $\varepsilon(NH_4^+)$ curve (the "S"-shaped curve, referred to as "S curve" hereafter) is plotted against pH based on the mean T (10 °C), AWC (100 μg m^{-3}), and $\frac{\gamma_{H^+}}{\gamma_{NH_4^+}}$ (2.4) during the haze period. Observation-based $\varepsilon(NH_4^+)$ as a function of pH with varying T and AWC is also shown. Clearly, the observational $\varepsilon(NH_4^+)$ data points are relatively well constrained by the theoretical equation, suggestive of reasonable judgment that $\varepsilon(NH_4^+)$ is controlled by T, AWC, pH, and $\frac{\gamma_{H^+}}{\gamma_{NH_4^+}}$. Under the condition of mean pH (4.6 ± 0.3) during the winter haze period, the S curve derives $\varepsilon(NH_4^+)$ of 0.3, around three-quarters of the mean measured $\varepsilon(NH_4^+)$ (0.4 ± 0.1). Earlier works have also observed a higher particle phase fraction than the Henry's law constants predicted for water-soluble aerosol components (Arellanes et al., 2006; Hennigan et al., 2008; Shen et al., 2018). Another possible factor contributing to the underestimation of $\varepsilon(NH_4^+)$ is the unaccounted effect from organic species, whose role in driving the SNA formation is thought to be significant (Silvern et al., 2017). The organics have been found to account for

Table 2. The summer and winter mean ($\pm 1\sigma$) $\varepsilon(NH_4^+)$, pH, T, activity coefficients ratio of $\frac{\gamma_{H^+}}{\gamma_{NH_4^+}}$, and NH_3 ($\mu g\,m^{-3}$) during the haze period.

	$\varepsilon(NH_4^+)$	AWC	pH	NH_3	$\frac{\gamma_{H^+}}{\gamma_{NH_4^+}}$	T
Summer	0.2 ± 0.1	79 ± 73	3.4 ± 0.5	40 ± 8	1.9 ± 0.9	29 ± 5
Winter	0.4 ± 0.1	115 ± 131	4.6 ± 0.3	20 ± 4	4.0 ± 4.7	5 ± 4

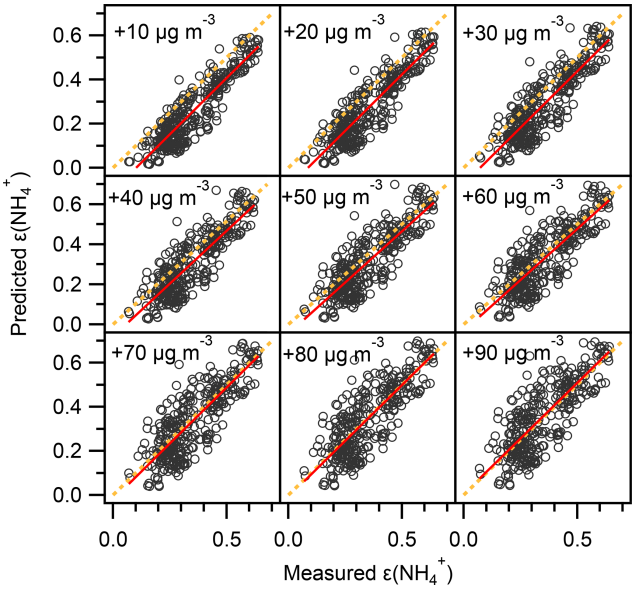

Figure 7. Comparison of predicted and measured $\varepsilon(NH_4^+)$. Note the predicted $\varepsilon(NH_4^+)$ was analytically calculated using Eq. (1) with input (i.e., pH, AWC, $\frac{\gamma_{H^+}}{\gamma_{NH_4^+}}$) taken from ISORROPIA II prediction, and the AWC has been increased by 10 and 20 to 90 $\mu g\,m^{-3}$ while other inputs are fixed. The orthogonal distance regression (ODR) fit line (red) and $y = x$ line (dashed orange) are shown for the clarity of the figure.

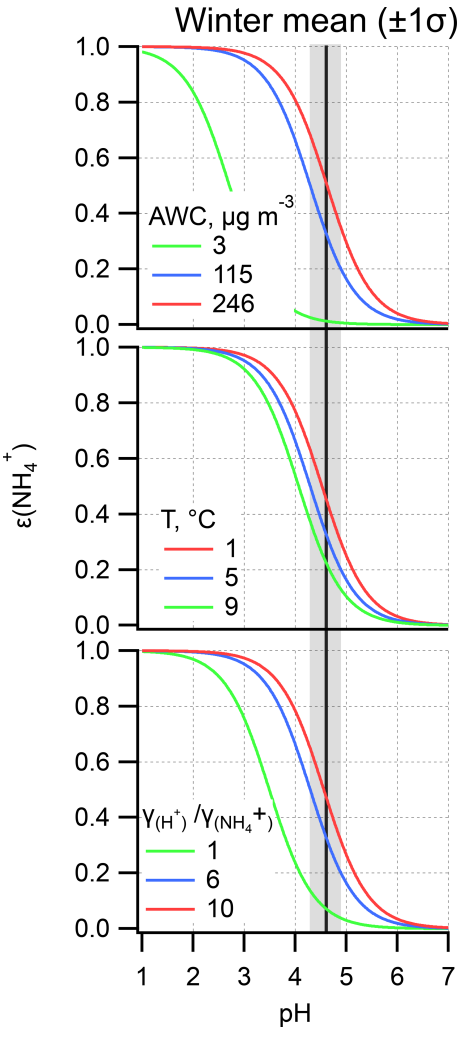

Figure 8. $\varepsilon(NH_4^+)$ as a function of pH during the winter haze period. Other variables are held constant at the mean value during the winter haze period, while varying only the AWC, T, and activity coefficients ratio of $\frac{\gamma_{H^+}}{\gamma_{NH_4^+}}$. Shaded dark areas indicate the winter haze mean pH together with 1 standard deviation ($\pm 1\sigma$). The areas between the green and red line represent the curve corresponding to mean $\pm 1\sigma$ – note that for AWC mean – 1σ yields a negative value; thus the minimum mass concentration (3 $\mu g\,m^{-3}$) was used.

35 % of AWC in the southeast USA (Guo et al., 2015); thus $\varepsilon(NH_4^+)$ would be enhanced by including organic aerosol. Since the mass concentration of organic aerosol was not available in this study, we did a sensitivity analysis by increasing the AWC by 10 and 20 to 90 $\mu g\,m^{-3}$ as shown in Fig. 7. The pH was not re-calculated using the new AWC because the co-existing organic aerosol altered pH in a complex way (Battaglia et al., 2019; Wang et al., 2018; Pye et al., 2020). For example, some organic acids increase aerosol acidity and thus decrease pH, whereas organic basics (e.g., amines) raise aerosol pH. We found that the best agreement between the predicted and measured $\varepsilon(NH_4^+)$ was achieved when we increase the AWC by roughly 90 $\mu g\,m^{-3}$, suggesting a nearly 48 % of AWC contributed by the organics. This result falls within the range from a recent report in north China according to which organics contribute to $30\,\% \pm 22\,\%$ of AWC (Jin et al., 2020); the result is slightly higher than

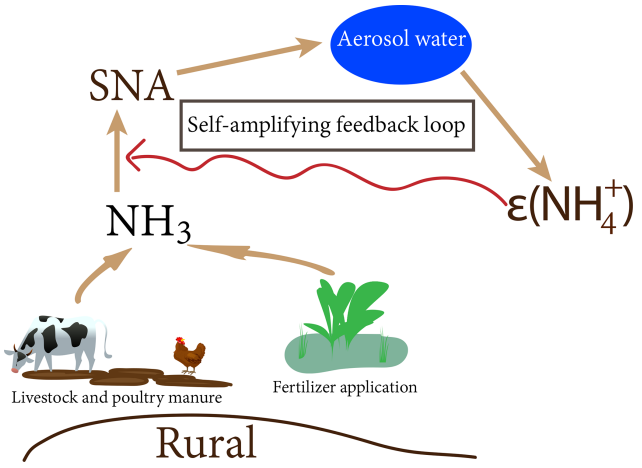

Figure 9. Schematic of self-amplifying feedback loop for SNA formation.

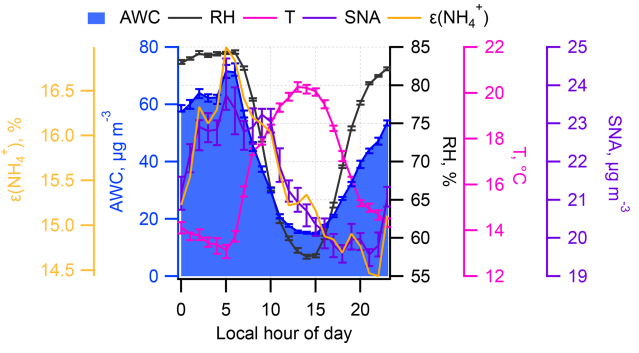

Figure 10. Annual mean diurnal pattern of $\varepsilon(NH_4^+)$, AWC, SNA, T, and RH.

at southeastern United States sites where organic aerosol-related water accounted for about 29 % to 39 % of total water (Guo et al., 2015) and in the eastern Mediterranean where about 27.5 % of total aerosol water resulted from organics (Bougiatioti et al., 2016). To quantitatively determine which parameter dominates the $\varepsilon(NH_4^+)$, the impact on $\varepsilon(NH_4^+)$ from an individual variable (i.e., T, AWC, pH, and $\frac{\gamma_{H^+}}{\gamma_{NH_4^+}}$) during the haze period in winter is assessed (Fig. 8). From a theoretical perspective, the decrease in pH and T and the increase in AWC and $\frac{\gamma_{H^+}}{\gamma_{NH_4^+}}$ would raise $\varepsilon(NH_4^+)$. For instance, in summertime, the lower $\varepsilon(NH_4^+)$ (Fig. 4) is mainly due to higher T that shifts the equilibrium to the gas phase; thus there is higher NH_3 ($40 \pm 8\,\mu g\,m^{-3}$) while lower NH_4^+ was observed. Likewise, in wintertime, the lower T facilitates the residence of NH_4^+ in the particle phase rather than the gas phase (NH_3: $20 \pm 4\,\mu g\,m^{-3}$), resulting in higher $\varepsilon(NH_4^+)$.

On the basis of the S curve (Fig. 8), each 0.1 unit change in $\varepsilon(NH_4^+)$ can be caused by approximately 5 °C, 75 $\mu g\,m^{-3}$, 0.3, and a 2-unit change in T, AWC, pH, and $\frac{\gamma_{H^+}}{\gamma_{NH_4^+}}$, respectively. Actually, T, pH, and $\frac{\gamma_{H^+}}{\gamma_{NH_4^+}}$ are within a relatively narrow range during the winter haze period (Table 2), suggesting the variation in these parameters should not result in the significant change in $\varepsilon(NH_4^+)$. By contrast, AWC fluctuates greatly during the study period (Table 2). Therefore, AWC should be the key factor regulating $\varepsilon(NH_4^+)$. It is well established that AWC is a function of RH and atmospheric aerosol compositions (Pilinis et al., 1989; Wu et al., 2018; Nguyen et al., 2016; Hodas et al., 2014). AWC has also been known to promote secondary organic aerosol formation by providing an aqueous medium for the uptake of reactive gases, gas-to-particle partitioning, and the subsequent chemical processing (McNeill, 2015; McNeill et al., 2012; Tan et al., 2009; Xu et al., 2017b).

The winter haze pH in this study was ∼ 3 units higher than that of the southeastern United States summer campaign (Nah et al., 2018; Guo et al., 2015, 2017a; Xu et al., 2017a), but close to that of 3.7 in rural Europe (Guo et al., 2018) and 4.2 in the North China Plain (Liu et al., 2017), where NH_3-rich conditions are prevalent. AWC may act as the major factor because greater AWC dilute the $[H^+]$ and raises the pH. The AWC during the haze period ($82 \pm 105\,\mu g\,m^{-3}$) was much higher than that during the non-haze period ($32 \pm 41\,\mu g\,m^{-3}$).

3.4 A possible self-amplifying feedback mechanism

Given that AWC is a function of RH and SNA, a conceptual model of how AWC controls $\varepsilon(NH_4^+)$ can be illustrated by a self-amplifying feedback loop (Fig. 9). The formation of SNA is initiated by gas-particle conversion of NH_3. Under certain meteorological conditions such as high RH and a shallow planetary boundary layer, SNA is subject to moisture uptake and results in the increases in AWC. The enhanced aerosol water dilutes the vapor pressure of semi-volatile species (i.e., nitrate, ammonium, and chloride) above the particle, and driving semi-volatile species continue to condense (Topping et al., 2013). Based on the discussions above, the increase in AWC would further raise $\varepsilon(NH_4^+)$, leading to a more efficient transformation of NH_3 as SNA.

Figure 10 shows the yearly mean diurnal variation in $\varepsilon(NH_4^+)$, AWC, and SNA along with T and RH. Apparently, SNA tracked well with $\varepsilon(NH_4^+)$ and AWC, especially over the nighttime. The not well-correlated track between SNA and AWC and $\varepsilon(NH_4^+)$ during the daytime (08:00–16:00 LT) can be ascribed to the photochemical reactions that lead to SNA formation. The good correlation between SNA and AWC and $\varepsilon(NH_4^+)$ demonstrated in Fig. 10 support the proposed self-amplifying feedback loop in SNA formation.

4 Conclusions

Our results demonstrate that $\varepsilon(NH_4^+)$, rather than NH_3 concentrations, plays a critical role in driving haze formation in the agricultural NH_3-emitting regions. Based on the S

curve calculation, we have unraveled that AWC is the major factor controlling $\varepsilon(NH_4^+)$. Upon analyzing the cross-correlations between AWC, $\varepsilon(NH_4^+)$, and SNA, we proposed a self-amplifying feedback mechanism of SNA formation that is associated with AWC and $\varepsilon(NH_4^+)$. This positive feedback cycle is likely to occur in other rural regions where high agricultural NH_3 emissions are prevalent.

We have shown that high NH_3 concentrations may not necessarily lead to strong SNA formation, particularly in agriculture-intensive areas, e.g., the North China Plain (NCP) and the extensive farming lands in eastern China where the high NH_3 levels are still unregulated and increasing (Meng et al., 2018; Warner et al., 2017). Although Liu et al. (2019) have predicted that $PM_{2.5}$ can be slashed by 11 %–17 % when there is a 50 % reduction in NH_3 by the agricultural sector and a 15 % mitigation of NO_x and SO_2 emissions was achieved, a recent study has demonstrated that only when aerosol pH drops below 3.0, would the NH_3 reduction have been expected to have mitigation effects (Guo et al., 2018). The winter haze pH (4.6 ± 0.3) in this study was mostly between 4–5. Our results thus imply that NH_3 alone may not be an effective solution to tackle air pollution in these regions.

Data availability. The data presented in this paper are available upon request from the corresponding author (huangkan@fudan.edu.cn).

Supplement. The supplement related to this article is available online at: https://doi.org/10.5194/acp-20-7259-2020-supplement.

Author contributions. JX and KH conceived the study. JX, JiaChen, and KH performed data analysis and wrote the paper. All authors contributed to the review of the paper.

Competing interests. The authors declare that they have no conflict of interest.

Special issue statement. This article is part of the special issue "Multiphase chemistry of secondary aerosol formation under severe haze". It is not associated with a conference.

Acknowledgements. We sincerely thank SEMC for maintaining the Chongming Dongtan supersite. We also thank the handling editor and three reviewers for providing the insightful comments and suggestions. We are grateful to Rodney Weber for helpful discussions.

Financial support. The authors acknowledge support of the National Key R&D Program of China (2018YFC0213105), the National Science Foundation of China (grant no. 91644105), and the Natural Science Foundation of Shanghai (18230722600, 19ZR1421100). Jian Xu acknowledge project funding by the China Postdoctoral Science Foundation (2019M651365).

Review statement. This paper was edited by Jian Wang and reviewed by three anonymous referees.

References

ApSimon, H. M., Kruse, M., and Bell, J. N. B.: Ammonia emissions and their role in acid deposition, Atmos. Environ., 21, 1939–1946, https://doi.org/10.1016/0004-6981(87)90154-5, 1987.

Arellanes, C., Paulson, S. E., Fine, P. M., and Sioutas, C.: Exceeding of Henry's Law by Hydrogen Peroxide Associated with Urban Aerosols, Environ. Sci. Technol., 40, 4859–4866, https://doi.org/10.1021/es0513786, 2006.

Ball, S. M., Hanson, D. R., Eisele, F. L., and McMurry, P. H.: Laboratory studies of particle nucleation: Initial results for H_2SO_4, H_2O, and NH_3 vapors, J. Geophys. Res.-Atmos., 104, 23709–23718, https://doi.org/10.1029/1999JD900411, 1999.

Battaglia Jr., M. A., Weber, R. J., Nenes, A., and Hennigan, C. J.: Effects of water-soluble organic carbon on aerosol pH, Atmos. Chem. Phys., 19, 14607–14620, https://doi.org/10.5194/acp-19-14607-2019, 2019.

Benner, W. H., Ogorevc, B., and Novakov, T.: Oxidation of SO_2 in thin water films containing NH_3, Atmos. Environ. A, 26, 1713–1723, https://doi.org/10.1016/0960-1686(92)90069-W, 1992.

Bougiatioti, A., Nikolaou, P., Stavroulas, I., Kouvarakis, G., Weber, R., Nenes, A., Kanakidou, M., and Mihalopoulos, N.: Particle water and pH in the eastern Mediterranean: source variability and implications for nutrient availability, Atmos. Chem. Phys., 16, 4579–4591, https://doi.org/10.5194/acp-16-4579-2016, 2016.

Chang, Y., Zou, Z., Deng, C., Huang, K., Collett, J. L., Lin, J., and Zhuang, G.: The importance of vehicle emissions as a source of atmospheric ammonia in the megacity of Shanghai, Atmos. Chem. Phys., 16, 3577–3594, https://doi.org/10.5194/acp-16-3577-2016, 2016.

Cheng, Y., Zheng, G., Wei, C., Mu, Q., Zheng, B., Wang, Z., Gao, M., Zhang, Q., He, K., Carmichael, G., Pöschl, U., and Su, H.: Reactive nitrogen chemistry in aerosol water as a source of sulfate during haze events in China, Sci. Adv., 2, e1601530, https://doi.org/10.1126/sciadv.1601530, 2016.

Clegg, S. L., Brimblecombe, P., and Wexler, A. S.: Thermodynamic Model of the System H^+-NH_4^+-SO_4^{2-}-NO_3^--H_2O at Tropospheric Temperatures, The J. Phys. Chem. A, 102, 2137–2154, https://doi.org/10.1021/jp973042r, 1998.

Coffman, D. J. and Hegg, D. A.: A preliminary study of the effect of ammonia on particle nucleation in the marine boundary layer, J. Geophys. Res.-Atmos., 100, 7147–7160, https://doi.org/10.1029/94JD03253, 1995.

Erisman, J. W., Sutton, M. A., Galloway, J., Klimont, Z., and Winiwarter, W.: How a century of ammonia synthesis changed the world, Nat. Geosci., 1, 636–639, https://doi.org/10.1038/ngeo325, 2008.

Fan, M., Shen, J., Yuan, L., Jiang, R., Chen, X., Davies, W. J., and Zhang, F.: Improving crop productivity and resource use efficiency to ensure food security and en-

vironmental quality in China, J. Exp. Bot., 63, 13–24, https://doi.org/10.1093/jxb/err248, 2011.

Fang, X., Shen, G., Xu, C., Qian, X., Li, J., Zhao, Z., Yu, S., and Zhu, C.: Agricultural ammonia emission inventory and its distribution characteristics in Shanghai, Acta Agriculturae Zhejiangensis, 27, 2177–2185, 2015 (in Chinese).

Fountoukis, C. and Nenes, A.: ISORROPIA II: a computationally efficient thermodynamic equilibrium model for K^+-Ca^{2+}–Mg^{2+}-NH_4^+-Na^+-SO_4^{2-}-NO_3^--Cl^--H_2O aerosols, Atmos. Chem. Phys., 7, 4639–4659, https://doi.org/10.5194/acp-7-4639-2007, 2007.

Fu, X., Wang, S., Xing, J., Zhang, X., Wang, T., and Hao, J.: Increasing Ammonia Concentrations Reduce the Effectiveness of Particle Pollution Control Achieved via SO_2 and NO_X Emissions Reduction in East China, Environ. Sci. Technol. Lett., 4, 221–227, https://doi.org/10.1021/acs.estlett.7b00143, 2017.

Gong, L., Lewicki, R., Griffin, R. J., Tittel, F. K., Lonsdale, C. R., Stevens, R. G., Pierce, J. R., Malloy, Q. G. J., Travis, S. A., Bobmanuel, L. M., Lefer, B. L., and Flynn, J. H.: Role of atmospheric ammonia in particulate matter formation in Houston during summertime, Atmos. Environ., 77, 893–900, https://doi.org/10.1016/j.atmosenv.2013.04.079, 2013.

Guo, H., Xu, L., Bougiatioti, A., Cerully, K. M., Capps, S. L., Hite Jr., J. R., Carlton, A. G., Lee, S.-H., Bergin, M. H., Ng, N. L., Nenes, A., and Weber, R. J.: Fine-particle water and pH in the southeastern United States, Atmos. Chem. Phys., 15, 5211–5228, https://doi.org/10.5194/acp-15-5211-2015, 2015.

Guo, H., Liu, J., Froyd, K. D., Roberts, J. M., Veres, P. R., Hayes, P. L., Jimenez, J. L., Nenes, A., and Weber, R. J.: Fine particle pH and gas–particle phase partitioning of inorganic species in Pasadena, California, during the 2010 CalNex campaign, Atmos. Chem. Phys., 17, 5703–5719, https://doi.org/10.5194/acp-17-5703-2017, 2017a.

Guo, H., Weber, R. J., and Nenes, A.: High levels of ammonia do not raise fine particle pH sufficiently to yield nitrogen oxide-dominated sulfate production, Sci. Rep., 7, 12109, https://doi.org/10.1038/s41598-017-11704-0, 2017b.

Guo, H., Otjes, R., Schlag, P., Kiendler-Scharr, A., Nenes, A., and Weber, R. J.: Effectiveness of ammonia reduction on control of fine particle nitrate, Atmos. Chem. Phys., 18, 12241–12256, https://doi.org/10.5194/acp-18-12241-2018, 2018.

Hennigan, C. J., Bergin, M. H., Dibb, J. E., and Weber, R. J.: Enhanced secondary organic aerosol formation due to water uptake by fine particles, Geophys. Res. Lett., 35, L18801, https://doi.org/10.1029/2008GL035046, 2008.

Hodas, N., Sullivan, A. P., Skog, K., Keutsch, F. N., Collett, J. L., Decesari, S., Facchini, M. C., Carlton, A. G., Laaksonen, A., and Turpin, B. J.: Aerosol Liquid Water Driven by Anthropogenic Nitrate: Implications for Lifetimes of Water-Soluble Organic Gases and Potential for Secondary Organic Aerosol Formation, Environ. Sci. Technol., 48, 11127–11136, https://doi.org/10.1021/es5025096, 2014.

Huang, C., Chen, C. H., Li, L., Cheng, Z., Wang, H. L., Huang, H. Y., Streets, D. G., Wang, Y. J., Zhang, G. F., and Chen, Y. R.: Emission inventory of anthropogenic air pollutants and VOC species in the Yangtze River Delta region, China, Atmos. Chem. Phys., 11, 4105–4120, https://doi.org/10.5194/acp-11-4105-2011, 2011.

Huang, R.-J., Zhang, Y., Bozzetti, C., Ho, K.-F., Cao, J.-J., Han, Y., Daellenbach, K. R., Slowik, J. G., Platt, S. M., Canonaco, F., Zotter, P., Wolf, R., Pieber, S. M., Bruns, E. A., Crippa, M., Ciarelli, G., Piazzalunga, A., Schwikowski, M., Abbaszade, G., Schnelle-Kreis, J., Zimmermann, R., An, Z., Szidat, S., Baltensperger, U., Haddad, I. E., and Prevot, A. S. H.: High secondary aerosol contribution to particulate pollution during haze events in China, Nature, 514, 218–222, https://doi.org/10.1038/nature13774, 2014.

Jin, X., Wang, Y., Li, Z., Zhang, F., Xu, W., Sun, Y., Fan, X., Chen, G., Wu, H., Ren, J., Wang, Q., and Cribb, M.: Significant contribution of organics to aerosol liquid water content in winter in Beijing, China, Atmos. Chem. Phys., 20, 901–914, https://doi.org/10.5194/acp-20-901-2020, 2020.

Kang, Y., Liu, M., Song, Y., Huang, X., Yao, H., Cai, X., Zhang, H., Kang, L., Liu, X., Yan, X., He, H., Zhang, Q., Shao, M., and Zhu, T.: High-resolution ammonia emissions inventories in China from 1980 to 2012, Atmos. Chem. Phys., 16, 2043–2058, https://doi.org/10.5194/acp-16-2043-2016, 2016.

Kirkby, J., Curtius, J., Almeida, J., Dunne, E., Duplissy, J., Ehrhart, S., Franchin, A., Gagné, S., Ickes, L., Kürten, A., Kupc, A., Metzger, A., Riccobono, F., Rondo, L., Schobesberger, S., Tsagkogeorgas, G., Wimmer, D., Amorim, A., Bianchi, F., Breitenlechner, M., David, A., Dommen, J., Downard, A., Ehn, M., Flagan, R. C., Haider, S., Hansel, A., Hauser, D., Jud, W., Junninen, H., Kreissl, F., Kvashin, A., Laaksonen, A., Lehtipalo, K., Lima, J., Lovejoy, E. R., Makhmutov, V., Mathot, S., Mikkilä, J., Minginette, P., Mogo, S., Nieminen, T., Onnela, A., Pereira, P., Petäjä, T., Schnitzhofer, R., Seinfeld, J. H., Sipilä, M., Stozhkov, Y., Stratmann, F., Tomé, A., Vanhanen, J., Viisanen, Y., Vrtala, A., Wagner, P. E., Walther, H., Weingartner, E., Wex, H., Winkler, P. M., Carslaw, K. S., Worsnop, D. R., Baltensperger, U., and Kulmala, M.: Role of sulphuric acid, ammonia and galactic cosmic rays in atmospheric aerosol nucleation, Nature, 476, 429, https://doi.org/10.1038/nature10343, 2011.

Kong, L., Yang, Y., Zhang, S., Zhao, X., Du, H., Fu, H., Zhang, S., Cheng, T., Yang, X., and Chen, J.: Observations of linear dependence between sulfate and nitrate in atmospheric particles, J. Geophys. Res.-Atmos., 119, 341–361, https://doi.org/10.1002/2013JD020222, 2014.

Lamarque, J.-F., Bond, T. C., Eyring, V., Granier, C., Heil, A., Klimont, Z., Lee, D., Liousse, C., Mieville, A., Owen, B., Schultz, M. G., Shindell, D., Smith, S. J., Stehfest, E., Van Aardenne, J., Cooper, O. R., Kainuma, M., Mahowald, N., McConnell, J. R., Naik, V., Riahi, K., and van Vuuren, D. P.: Historical (1850–2000) gridded anthropogenic and biomass burning emissions of reactive gases and aerosols: methodology and application, Atmos. Chem. Phys., 10, 7017–7039, https://doi.org/10.5194/acp-10-7017-2010, 2010.

Liu, M., Song, Y., Zhou, T., Xu, Z., Yan, C., Zheng, M., Wu, Z., Hu, M., Wu, Y., and Zhu, T.: Fine particle pH during severe haze episodes in northern China, Geophys. Res. Lett., 44, 5213–5221, https://doi.org/10.1002/2017GL073210, 2017.

Liu, M., Huang, X., Song, Y., Tang, J., Cao, J., Zhang, X., Zhang, Q., Wang, S., Xu, T., Kang, L., Cai, X., Zhang, H., Yang, F., Wang, H., Yu, J. Z., Lau, A. K. H., He, L., Huang, X., Duan, L., Ding, A., Xue, L., Gao, J., Liu, B., and Zhu, T.: Ammonia emission control in China would mitigate haze pollution and nitrogen deposition, but worsen acid rain, P. Natl. Acad. Sci. USA, 116, 7760–7765, https://doi.org/10.1073/pnas.1814880116, 2019.

McNeill, V. F.: Aqueous Organic Chemistry in the Atmosphere: Sources and Chemical Processing of Organic Aerosols, Environ. Sci. Technol., 49, 1237–1244, https://doi.org/10.1021/es5043707, 2015.

McNeill, V. F., Woo, J. L., Kim, D. D., Schwier, A. N., Wannell, N. J., Sumner, A. J., and Barakat, J. M.: Aqueous-Phase Secondary Organic Aerosol and Organosulfate Formation in Atmospheric Aerosols: A Modeling Study, Environ. Sci. Technol., 46, 8075–8081, https://doi.org/10.1021/es3002986, 2012.

Meng, Z., Xu, X., Lin, W., Ge, B., Xie, Y., Song, B., Jia, S., Zhang, R., Peng, W., Wang, Y., Cheng, H., Yang, W., and Zhao, H.: Role of ambient ammonia in particulate ammonium formation at a rural site in the North China Plain, Atmos. Chem. Phys., 18, 167–184, https://doi.org/10.5194/acp-18-167-2018, 2018.

Na, K., Song, C., Switzer, C., and Cocker, D. R.: Effect of Ammonia on Secondary Organic Aerosol Formation from α-Pinene Ozonolysis in Dry and Humid Conditions, Environ. Sci. Technol., 41, 6096–6102, https://doi.org/10.1021/es061956y, 2007.

Nah, T., Guo, H., Sullivan, A. P., Chen, Y., Tanner, D. J., Nenes, A., Russell, A., Ng, N. L., Huey, L. G., and Weber, R. J.: Characterization of aerosol composition, aerosol acidity, and organic acid partitioning at an agriculturally intensive rural southeastern US site, Atmos. Chem. Phys., 18, 11471–11491, https://doi.org/10.5194/acp-18-11471-2018, 2018.

Nguyen, T. K. V., Zhang, Q., Jimenez, J. L., Pike, M., and Carlton, A. G.: Liquid Water: Ubiquitous Contributor to Aerosol Mass, Environ. Sci. Technol. Lett., 3, 257–263, https://doi.org/10.1021/acs.estlett.6b00167, 2016.

Nowak, J. B., Neuman, J. A., Bahreini, R., Brock, C. A., Middlebrook, A. M., Wollny, A. G., Holloway, J. S., Peischl, J., Ryerson, T. B., and Fehsenfeld, F. C.: Airborne observations of ammonia and ammonium nitrate formation over Houston, Texas, J. Geophys. Res.-Atmos., 115, D22304, https://doi.org/10.1029/2010JD014195, 2010.

Nowak, J. B., Neuman, J. A., Bahreini, R., Middlebrook, A. M., Holloway, J. S., McKeen, S. A., Parrish, D. D., Ryerson, T. B., and Trainer, M.: Ammonia sources in the California South Coast Air Basin and their impact on ammonium nitrate formation, Geophys. Res. Lett., 39, L07804, https://doi.org/10.1029/2012GL051197, 2012.

Noziere, B., Dziedzic, P., and Cordova, A.: Inorganic ammonium salts and carbonate salts are efficient catalysts for aldol condensation in atmospheric aerosols, Phys. Chem. Chem. Phys., 12, 3864–3872, https://doi.org/10.1039/B924443C, 2010.

Ortiz-Montalvo, D. L., Häkkinen, S. A. K., Schwier, A. N., Lim, Y. B., McNeill, V. F., and Turpin, B. J.: Ammonium Addition (and Aerosol pH) Has a Dramatic Impact on the Volatility and Yield of Glyoxal Secondary Organic Aerosol, Environ. Sci. Technol., 48, 255–262, https://doi.org/10.1021/es4035667, 2013.

Pan, Y., Tian, S., Zhao, Y., Zhang, L., Zhu, X., Gao, J., Huang, W., Zhou, Y., Song, Y., Zhang, Q., and Wang, Y.: Identifying Ammonia Hotspots in China Using a National Observation Network, Environ. Sci. Technol., 52, 3926–3934, https://doi.org/10.1021/acs.est.7b05235, 2018.

Park, R. S., Lee, S., Shin, S.-K., and Song, C. H.: Contribution of ammonium nitrate to aerosol optical depth and direct radiative forcing by aerosols over East Asia, Atmos. Chem. Phys., 14, 2185–2201, https://doi.org/10.5194/acp-14-2185-2014, 2014.

Paulot, F., Paynter, D., Ginoux, P., Naik, V., Whitburn, S., Van Damme, M., Clarisse, L., Coheur, P. F., and Horowitz, L. W.: Gas-aerosol partitioning of ammonia in biomass burning plumes: Implications for the interpretation of spaceborne observations of ammonia and the radiative forcing of ammonium nitrate, Geophys. Res. Lett., 44, 8084–8093, https://doi.org/10.1002/2017GL074215, 2017.

Peng, G., Jie, W., Luyang, J., and Le, Y.: FROM-GLC 2015 v0.1, figshare, https://doi.org/10.6084/m9.figshare.5362774.v2, 2018.

Phan, N.-T., Kim, K.-H., Shon, Z.-H., Jeon, E.-C., Jung, K., and Kim, N.-J.: Analysis of ammonia variation in the urban atmosphere, Atmos. Environ., 65, 177–185, https://doi.org/10.1016/j.atmosenv.2012.10.049, 2013.

Pilinis, C., Seinfeld, J. H., and Grosjean, D.: Water content of atmospheric aerosols, Atmos. Environ., 23, 1601–1606, https://doi.org/10.1016/0004-6981(89)90419-8, 1989.

Plautz, J.: Piercing the haze, Science, 361, 1060–1063, 2018.

Pye, H. O. T., Nenes, A., Alexander, B., Ault, A. P., Barth, M. C., Clegg, S. L., Collett Jr., J. L., Fahey, K. M., Hennigan, C. J., Herrmann, H., Kanakidou, M., Kelly, J. T., Ku, I.-T., McNeill, V. F., Riemer, N., Schaefer, T., Shi, G., Tilgner, A., Walker, J. T., Wang, T., Weber, R., Xing, J., Zaveri, R. A., and Zuend, A.: The acidity of atmospheric particles and clouds, Atmos. Chem. Phys., 20, 4809–4888, https://doi.org/10.5194/acp-20-4809-2020, 2020.

Robarge, W. P., Walker, J. T., McCulloch, R. B., and Murray, G.: Atmospheric concentrations of ammonia and ammonium at an agricultural site in the southeast United States, Atmos. Environ., 36, 1661–1674, https://doi.org/10.1016/S1352-2310(02)00171-1, 2002.

Schiferl, L. D., Heald, C. L., Nowak, J. B., Holloway, J. S., Neuman, J. A., Bahreini, R., Pollack, I. B., Ryerson, T. B., Wiedinmyer, C., and Murphy, J. G.: An investigation of ammonia and inorganic particulate matter in California during the CalNex campaign, J. Geophys. Res.-Atmos., 119, 1883–1902, https://doi.org/10.1002/2013JD020765, 2014.

Seinfeld, J. H. and Pandis, S. N.: Atmospheric chemistry and physics: from air pollution to climate change, Wiley, 1232 pp., 2012.

Shen, H., Chen, Z., Li, H., Qian, X., Qin, X., and Shi, W.: Gas-Particle Partitioning of Carbonyl Compounds in the Ambient Atmosphere, Environ. Sci. Technol., 52, 10997–11006, https://doi.org/10.1021/acs.est.8b01882, 2018.

Shen, J., Liu, X., Zhang, Y., Fangmeier, A., Goulding, K., and Zhang, F.: Atmospheric ammonia and particulate ammonium from agricultural sources in the North China Plain, Atmos. Environ., 45, 5033–5041, https://doi.org/10.1016/j.atmosenv.2011.02.031, 2011.

Silvern, R. F., Jacob, D. J., Kim, P. S., Marais, E. A., Turner, J. R., Campuzano-Jost, P., and Jimenez, J. L.: Inconsistency of ammonium–sulfate aerosol ratios with thermodynamic models in the eastern US: a possible role of organic aerosol, Atmos. Chem. Phys., 17, 5107–5118, https://doi.org/10.5194/acp-17-5107-2017, 2017.

Stewart, W. M., Dibb, D. W., Johnston, A. E., and Smyth, T. J.: The Contribution of Commercial Fertilizer Nutrients to Food Production, Agro. J., 97, 1–6, https://doi.org/10.2134/agronj2005.0001, 2005.

Sun, K., Tao, L., Miller, D. J., Pan, D., Golston, L. M., Zondlo, M. A., Griffin, R. J., Wallace, H. W., Leong, Y. J., Yang,

M. M., Zhang, Y., Mauzerall, D. L., and Zhu, T.: Vehicle Emissions as an Important Urban Ammonia Source in the United States and China, Environ. Sci. Technol., 51, 2472–2481, https://doi.org/10.1021/acs.est.6b02805, 2017.

Sun, Y., Jiang, Q., Wang, Z., Fu, P., Li, J., Yang, T., and Yin, Y.: Investigation of the sources and evolution processes of severe haze pollution in Beijing in January 2013, J. Geophys. Res.-Atmos., 119, 4380–4398, https://doi.org/10.1002/2014JD021641, 2014.

Tan, Y., Perri, M. J., Seitzinger, S. P., and Turpin, B. J.: Effects of Precursor Concentration and Acidic Sulfate in Aqueous Glyoxal-OH Radical Oxidation and Implications for Secondary Organic Aerosol, Environ. Sci. Technol., 43, 8105–8112, https://doi.org/10.1021/es901742f, 2009.

Topping, D., Connolly, P., and McFiggans, G.: Cloud droplet number enhanced by co-condensation of organic vapours, Nat. Geosci., 6, 443–446, https://doi.org/10.1038/ngeo1809, 2013.

Turšič, J., Berner, A., Podkrajšek, B., and Grgić, I.: Influence of ammonia on sulfate formation under haze conditions, Atmos. Environ., 38, 2789–2795, https://doi.org/10.1016/j.atmosenv.2004.02.036, 2004.

Wang, G., Zhang, R., Gomez, M. E., Yang, L., Levy Zamora, M., Hu, M., Lin, Y., Peng, J., Guo, S., Meng, J., Li, J., Cheng, C., Hu, T., Ren, Y., Wang, Y., Gao, J., Cao, J., An, Z., Zhou, W., Li, G., Wang, J., Tian, P., Marrero-Ortiz, W., Secrest, J., Du, Z., Zheng, J., Shang, D., Zeng, L., Shao, M., Wang, W., Huang, Y., Wang, Y., Zhu, Y., Li, Y., Hu, J., Pan, B., Cai, L., Cheng, Y., Ji, Y., Zhang, F., Rosenfeld, D., Liss, P. S., Duce, R. A., Kolb, C. E., and Molina, M. J.: Persistent sulfate formation from London Fog to Chinese haze, P. Natl. Acad. Sci. USA, 113, 13630–13635, https://doi.org/10.1073/pnas.1616540113, 2016.

Wang, G., Zhang, F., Peng, J., Duan, L., Ji, Y., Marrero-Ortiz, W., Wang, J., Li, J., Wu, C., Cao, C., Wang, Y., Zheng, J., Secrest, J., Li, Y., Wang, Y., Li, H., Li, N., and Zhang, R.: Particle acidity and sulfate production during severe haze events in China cannot be reliably inferred by assuming a mixture of inorganic salts, Atmos. Chem. Phys., 18, 10123–10132, https://doi.org/10.5194/acp-18-10123-2018, 2018.

Wang, Q., Zhuang, G., Huang, K., Liu, T., Deng, C., Xu, J., Lin, Y., Guo, Z., Chen, Y., Fu, Q., Fu, J. S., and Chen, J.: Probing the severe haze pollution in three typical regions of China: Characteristics, sources and regional impacts, Atmos. Environ., 120, 76–88, https://doi.org/10.1016/j.atmosenv.2015.08.076, 2015a.

Wang, S., Nan, J., Shi, C., Fu, Q., Gao, S., Wang, D., Cui, H., Saiz-Lopez, A., and Zhou, B.: Atmospheric ammonia and its impacts on regional air quality over the megacity of Shanghai, China, Sci. Rep., 5, 15842, https://doi.org/10.1038/srep15842, 2015b.

Wang, Y., Zhang, Q. Q., He, K., Zhang, Q., and Chai, L.: Sulfate-nitrate-ammonium aerosols over China: response to 2000–2015 emission changes of sulfur dioxide, nitrogen oxides, and ammonia, Atmos. Chem. Phys., 13, 2635–2652, https://doi.org/10.5194/acp-13-2635-2013, 2013.

Warner, J. X., Dickerson, R. R., Wei, Z., Strow, L. L., Wang, Y., and Liang, Q.: Increased atmospheric ammonia over the world's major agricultural areas detected from space, Geophys. Res. Lett., 44, 2875–2884, https://doi.org/10.1002/2016GL072305, 2017.

Wei, L., Duan, J., Tan, J., Ma, Y., He, K., Wang, S., Huang, X., and Zhang, Y.: Gas-to-particle conversion of atmospheric ammonia and sampling artifacts of ammonium in spring of Beijing, Sci. China Earth Sci., 58, 345–355, https://doi.org/10.1007/s11430-014-4986-1, 2015.

Wells, M., Choularton, T. W., and Bower, K. N.: A modelling study of the interaction of ammonia with cloud, Atmos. Environ., 32, 359–363, https://doi.org/10.1016/S1352-2310(97)00199-4, 1998.

Wen, X., He, Z., and Zhang, Z.: Surveying and Evaluating of Land Environmental Quality and Monitoring of Basic Farmland Environmental Quality in Shanghai, Shanghai Land Resour., 32, 8–13, 2011 (in Chinese).

Wu, Y., Gu, B., Erisman, J. W., Reis, S., Fang, Y., Lu, X., and Zhang, X.: $PM_{2.5}$ pollution is substantially affected by ammonia emissions in China, Environ. Pollut., 218, 86–94, https://doi.org/10.1016/j.envpol.2016.08.027, 2016.

Wu, Z., Wang, Y., Tan, T., Zhu, Y., Li, M., Shang, D., Wang, H., Lu, K., Guo, S., Zeng, L., and Zhang, Y.: Aerosol liquid water driven by anthropogenic inorganic salts: Implying its key role in haze formation over the North China Plain, Environ. Sci. Technol. Lett., 5, 160–166, https://doi.org/10.1021/acs.estlett.8b00021, 2018.

Xu, L., Guo, H., Weber, R. J., and Ng, N. L.: Chemical Characterization of Water-Soluble Organic Aerosol in Contrasting Rural and Urban Environments in the Southeastern United States, Environ. Sci. Technol., 51, 78–88, https://doi.org/10.1021/acs.est.6b05002, 2017a.

Xu, W., Han, T., Du, W., Wang, Q., Chen, C., Zhao, J., Zhang, Y., Li, J., Fu, P., Wang, Z., Worsnop, D. R., and Sun, Y.: Effects of Aqueous-Phase and Photochemical Processing on Secondary Organic Aerosol Formation and Evolution in Beijing, China, Environ. Sci. Technol., 51, 762–770, https://doi.org/10.1021/acs.est.6b04498, 2017b.

Yang, X. and Fang, S.: Practices, perceptions, and implications of fertilizer use in East-Central China, Ambio, 44, 647–652, https://doi.org/10.1007/s13280-015-0639-7, 2015.

Yao, X., Yan Ling, T., Fang, M., and Chan, C. K.: Comparison of thermodynamic predictions for in situ pH in PM2.5, Atmos. Environ., 40, 2835–2844, https://doi.org/10.1016/j.atmosenv.2006.01.006, 2006.

Ye, X., Ma, Z., Zhang, J., Du, H., Chen, J., Chen, H., Yang, X., Gao, W., and Geng, F.: Important role of ammonia on haze formation in Shanghai, Environ. Res. Lett., 6, 024019, https://doi.org/10.1088/1748-9326/6/2/024019, 2011.

Zhang, L., Chen, Y., Zhao, Y., Henze, D. K., Zhu, L., Song, Y., Paulot, F., Liu, X., Pan, Y., Lin, Y., and Huang, B.: Agricultural ammonia emissions in China: reconciling bottom-up and top-down estimates, Atmos. Chem. Phys., 18, 339–355, https://doi.org/10.5194/acp-18-339-2018, 2018.

Zhang, R., Khalizov, A., Wang, L., Hu, M., and Xu, W.: Nucleation and growth of nanoparticles in the atmosphere, Chem. Rev., 112, 1957–2011, https://doi.org/10.1021/cr2001756, 2011.

Zhang, X., Wu, Y., Liu, X., Reis, S., Jin, J., Dragosits, U., Van Damme, M., Clarisse, L., Whitburn, S., Coheur, P.-F., and Gu, B.: Ammonia Emissions May Be Substantially Underestimated in China, Environ. Sci. Technol., 51, 12089–12096, https://doi.org/10.1021/acs.est.7b02171, 2017.